

PREDICTION OF VOID FRACTION UNCERTAINTY BANDS IN BWR FUEL BUNDLES USING THE CIAU METHODOLOGY

K. Leung*, A. Kovtonyuk, A. Petruzzi, F. D'Auria

Dipartimento di Ingegneria, Meccanica, Nucleare e della Produzione
Università di Pisa
Via Diotisalvi 2, 56100 Pisa, Italy

D. R. Novog

Department of Engineering Physics
McMaster University
1280 Main St. W., Hamilton, Canada

ABSTRACT

One of the tasks of the Boiling Water Reactor (BWR) Full-size-fine-mesh Bundle Test (BFBT) is to examine the derivation of uncertainty bounds on the void fraction of a BWR fuel bundle. A Code (with the capability of) Internal Assessment of Uncertainty (CIAU) was originally proposed by the University of Pisa as a means of deriving uncertainty bounds in Nuclear Power Plant (NPP) calculations based on the difference between simulated and experimental data. This paper demonstrates how the core of the CIAU methodology may be adapted to generate uncertainty bands around subchannel void fraction predictions made by RELAP5-3D. In three of the four cases tested, the experimental subchannel void fraction fell within the predicted uncertainty bounds over 98% of the time. The fourth case consisted of low pressure, power and flow boundary conditions which led to poor subchannel void accuracy. An accuracy analysis indicates that this particular case has a sample averaged bias error of 0.191, which is about one order of magnitude higher than the other three cases examined. A planar average taken over all of the subchannels shows that the differences between simulated and experimental voids are less than 0.05 (in absolute terms) in all four of the cases examined.

Key Words: thermalhydraulics, void fraction, BFBT, uncertainty, CIAU

1. INTRODUCTION

Accurate prediction of the void fraction distribution in fuel bundles has always been a difficult task for thermal-hydraulics codes. A lack of reliable full scale bundle data has been cited as one of the reasons that highly refined models are unavailable [1]. Between 1987 and 1995, the Nuclear Power Engineering Corporation (NUPEC) of Japan conducted a series of experiments on full sized mock-ups of Boiling Water Reactor (BWR) and Pressurized Water Reactor (PWR) fuel bundles. Using the state of the art techniques at the time, the researchers were able to make detailed high-resolution void fraction measurements under conditions similar to those found in

*McMaster University. Contact e-mail: leungk4@mcmaster.ca

an operational BWR [1]. A comprehensive database of the results was compiled and released for use in the Organization of Economic Cooperation and Development (OECD) / Nuclear Energy Agency (NEA) BWR Full-Size Fine-Mesh Bundle Test (BFBT) benchmark.

Exercise 4 – Phase 1 [2] of the benchmark assesses the different uncertainty analysis methodologies for predicting the uncertainty in the void fraction prediction. One of the methods being studied is the Code (with the capability of) Internal Assessment of Uncertainty (CIAU) proposed by the University of Pisa. This paper, will demonstrate how the basic principles behind CIAU may be adapted to generate uncertainty bands on void fraction predictions at a subchannel level. Specifically, RELAP5-3D will be used to simulate a series of tests run by NUPEC. The simulation results will be compared with the experimental data to generate a database of accuracy quantities from which uncertainty bounds may be derived. A statistical accuracy analysis of the cases examined will also provide a quantitative comparison of the nodalization performance.

2. TEST FACILITY

The NUPEC bundle test facility allows electrically heated BWR fuel-bundles constructed at full scale to be simulated. Results in this study focus only on the 4101-XX series of tests that utilize the bundle shown in Figure 1, while other characteristics of the facility are summarized in Table I. The bundle has a non-uniform power profile in the planar direction and a uniform profile in the axial direction.

Operating conditions including the bundle power, axial and planar power profile, inlet and outlet pressure, mass flow rate and the inlet subcooling were all measured and provided to the BFBT benchmark participants. The void fraction at the top of the heated section is measured on a subchannel basis by X-ray CT scanners which were determined to be accurate to $\pm 3\%$ of the given value, again, in absolute terms [1].

2.1. RELAP5-3D Nodalization

The University of Pisa (UNIPi) is conducting its assessment [3] for the benchmark using RELAP5-3D version 2.2.4 [4].

Table I. Test Facility and Fuel Bundle Parameters [1].

Parameter	Quantity
Maximum Power (MW)	12
Maximum Mass Flux (kg / m ² -s)	2130
Maximum Pressure (MPa)	10.3
Number of Fuel Rods	62
Rod Pitch (mm)	16.2
Fuel Rod Diameter (mm)	12.3
Number of Water Rods	1
Water Rod Diameter (mm)	34.0
Heated Length (mm)	3708

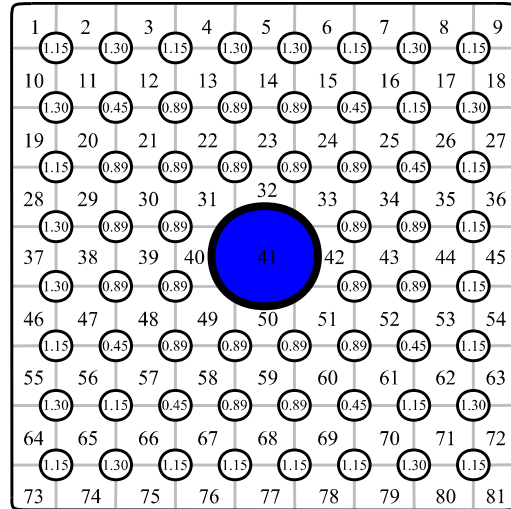


Figure 1. Cross sectional view of the fuel bundle with subchannel indices and relative rod power listed [1]. The shaded rod in the center is a water rod and is not heated.

The geometry of the active portion of the fuel bundle is modeled using the multi-dimensional (MULTI-D) component of the code, which represents a three-dimensional array of volumes. The UNIFI nodalization of the bundle represents the 80 subchannels as a 9×9 planar array with 12 axial levels, each 0.309 m in length. The central subchannel (#41 in Figure 1) represents the water rod and there is no flow rate from the surrounding subchannels towards the central one and vice versa. A code limitation that restricts the MULTI-D Component to a maximum of 999 nodes prevents a finer axial mesh from being used [3, 4]. The flow areas in both the lateral and axial directions are preserved.

Each fuel rod is independently modeled as four heat structures connected using a conduction enclosure and contains 12 axial levels. The experimental void fraction is recorded at the top of the heated section and is compared to the void in the top node in the simulated results. The simulated values represent the average void over the top 0.309 m of the heated section.

Boundary conditions such as inlet and outlet pressure, inlet fluid temperature and mass flow rate are imposed by utilizing the RELAP5 Time-Dependent Volumes and Junctions. Two-phase mass, momentum and energy equations are solved for the liquid/vapour flow.

3. METHODOLOGY

3.1. Accuracy Quantification

In order to assess the accuracy of the simulations, several quantities are derived in reference 2, and these are listed in Table II. For this study, the “sample averaged absolute bias error”, has been added as a metric since we have found that the simulated values (α^{code}) often straddle the experimental value (α^{exp}) causing the value of the bias error to be misleadingly small.

Table II. Accuracy Quantification Term Definitions [2].

Quantity	Definition
Planar Averaged Void Distribution	$\bar{\alpha}^{\text{code}} = \frac{1}{N} \sum_{n=1}^N \alpha_n^{\text{code}}$
Sample Averaged Bias Error	$\bar{\delta}^{\text{code}} = \frac{1}{N} \sum_{n=1}^N \frac{\alpha_n^{\text{code}} - \alpha_n^{\text{exp}}}{\alpha_n^{\text{exp}}}$
Sample Averaged Absolute Bias Error	$ \bar{\delta} ^{\text{code}} = \frac{1}{N} \sum_{n=1}^N \frac{ \alpha_n^{\text{code}} - \alpha_n^{\text{exp}} }{\alpha_n^{\text{exp}}}$
Maximum Bias Error	$\varepsilon^{\text{code}} = \max \left(\frac{\alpha_n^{\text{code}} - \alpha_n^{\text{exp}}}{\alpha_n^{\text{exp}}} \right)$
Standard Deviation	$\sigma^{\text{code}} = \sqrt{\frac{1}{N} \sum_{n=1}^N \left(\alpha_n^{\text{code}} - \bar{\alpha}^{\text{code}} \right)^2}$
Coverage Ratio	$\frac{\# \text{ of points where: } \left(\frac{\alpha_n^{\text{code}} - \alpha_n^{\text{exp}}}{\alpha_n^{\text{exp}}} \right) \leq \varepsilon^{\text{exp}}}{N}$

3.2. CIAU Methodology

CIAU was developed at UNIPI as a means of estimating the uncertainty bands in NPP transients by a qualified system code. In the context of the BFBT benchmark, a code based on the core concepts of the CIAU methodology was developed in order to estimate the uncertainty of the simulated void fraction in the fuel bundles.

The CIAU methodology assumes that all operational states of an NPP may be characterized as a combination of selected ‘driving quantities’ [5]. These driving quantities form the basis of a hypercube in n-dimensional Euclidian-space, and it is postulated that different combinations of these driving quantities will have inherently different associated uncertainties during the simulated transients. In essence, the methodology allows the uncertainty to be a function of the specific phenomena at a given time in the accident sequence depending on the specific combination of the driving quantities. In simulations of BWR transients, the CIAU methodology has established the driving quantities to be: upper plenum pressure, primary circuit mass inventory, cladding temperature, core power and downcomer level [5].

Since this portion of the BFBT benchmark focuses solely on the behaviour of a single fuel bundle at steady state, a different set of driving quantities must be derived. Four parameters are selected for characterizing the accuracy of the void in the BFBT simulations. They are: subchannel power to mass flux ratio, inlet pressure, inlet subcooling and the simulated void fraction in the subchannel. These driving quantities are normalized, subdivided into appropriate intervals and form the bases of the new hypercubes.

In order to take advantage of the quantity of data available, a RELAP5-3D calculation of the bundle was performed for each available set of experimental conditions. The void prediction for each subchannel is treated as an individual data point, with each case run providing up to 80 points for the database.

An Accuracy Quantity (AQ), defined in equation 1, is calculated for each data point. In the equation, Y_E and Y_S represent the experimental and simulated subchannel void fraction at the top of the active portion of each fuel bundle, while $\varepsilon = \pm 0.03 Y_E$ represents the experimental uncertainty provided in the BFBT specifications [2].

$$AQ = \begin{cases} \frac{Y_S - (Y_E + \varepsilon^+)}{Y_S} & (Y_E + \varepsilon^+) < Y_S \\ \frac{(Y_E - \varepsilon^-) - Y_S}{Y_S} & Y_S < (Y_E - \varepsilon^-) \\ 0 & (Y_E - \varepsilon^-) \leq Y_S \leq (Y_E + \varepsilon^+) \end{cases} \quad (1)$$

Each hypercube may contain the results of several tests. However, data points from one test can be spread over several hypercubes as the subchannels at the sides and corners of the bundle have different power to mass flux ratios than those in the center.

The dispersion of data points belonging to the same test in a hypercube is accounted for using equations 2 to 5. In the subsequent equations, superscript i denotes the index of the hypercube, j is the specific test and $f(k)$ represents the subchannel number within the hypercube i . When N_j^i points from test j are classified into hypercube i , the average and standard deviation are found for each test using equations 2 and 3.

$$\overline{AQ_j^i} = \sum_{k=1}^{N_j^i} \frac{AQ_{j,f(k)}^i}{N_j^i} \quad (2)$$

$$S_j^i = \frac{1}{AQ_j^i} \sqrt{\frac{\sum_{k=1}^{N_j^i} (AQ_{j,f(k)}^i - \overline{AQ_j^i})^2}{N_j^i - 1}} \quad (3)$$

It is obvious that $\sum_{i=1}^{Tot\ N.Hyp} N_j^i = 80$.

A weighting factor P_j for each test j in hypercube i is derived in equations 4 and 5. P_d represents experimental uncertainty in the test data, P_k is a weighting factor that accounts for the scaling of the test facility, and P_s is the weighting factor, which accounts for the dispersion of points in each test as calculated in equation 4, and N^i is the total number of tests inside the hypercube i . In the BFBT benchmark cases, $P_d = 0.03$ as provided by the specifications, and $P_k = 1$ since the tests were conducted at full scale.

$$P_s^i = \begin{cases} 1.0 - 0.9S_j^i & \text{if } 0.0 < S_j^i < 1.0 \\ 0.1 & \text{if } S_j^i \geq 1.0 \end{cases} \quad (4)$$

$$P_j^i = \frac{(Pd_j^i)(Pk_j^i)(Ps_j^i)}{\sum_{j=1}^{N^i} (Pd_j^i)(Pk_j^i)(Ps_j^i)} \quad (5)$$

The dispersion of the tests in a hypercube is accounted for using equations 6 and 7 which are the average and weighted standard deviations calculated over N^i tests in the hypercube i .

$$\overline{AQ^i} = \sum_{j=1}^{N^i} \frac{AQ_j^i}{N_j} \quad (6)$$

$$\sigma^i = \sqrt{\frac{\sum_{j=1}^{N^i} (P_j N^i |AQ_j^i - \overline{AQ^i}|)^2}{N^i - 1}} \quad (7)$$

When a simulation is performed, an estimate of the uncertainty band is made possible by using the statistical information contained in the associated hypercubes (Eq. 8).

$$U^i = \overline{AQ^i} + \left(\sum_{j=1}^{N^i} 2P_j^i S_j^i AQ_j^i \right) + (1.96\sigma^i) \quad (8)$$

Equation 9 predicts the bounds of a two-tailed 95% uncertainty band for the simulated void fraction α_{sim} .

$$\alpha_{band} = \alpha_{sim} \pm \alpha_{sim} \cdot U^i \quad (9)$$

4. RESULTS

Using data supplied from the BFBT benchmark database, 86 experimental runs were identified as being relevant to this study. The process conditions from these experimental runs were translated into boundary conditions in the input files, and each case was simulated in RELAP5-3D. Of the 86 tests simulated, 82 cases were used to derive the accuracy (AQ^i) and uncertainty (U^i) database, while the remaining 4 cases were isolated for performing the “external validation process” [5, 6] of the developed tool for carrying out the uncertainty analysis.

The same nodalization was used for all simulations, with only the relevant boundary conditions being varied. The test cases used in the uncertainty analysis are provided in Table III.

Uncertainty bounds are generated based on the uncertainty database, and applied to the predicted results in Figure 2 and Figure 3.

Table III. Boundary Conditions for uncertainty cases.

	Test			
	4101-02	4101-13	4101-69	4101-86
Inlet Pressure (MPa)	1.03	1.22	8.66	8.77
Mass Flux (kg/m²-s)	297.1	1614.7	395.8	1602.4
Power (MW)	0.32	4.46	0.23	4.62
Inlet Subcooling (kJ/kg)	53.3	92.5	52.5	54.2

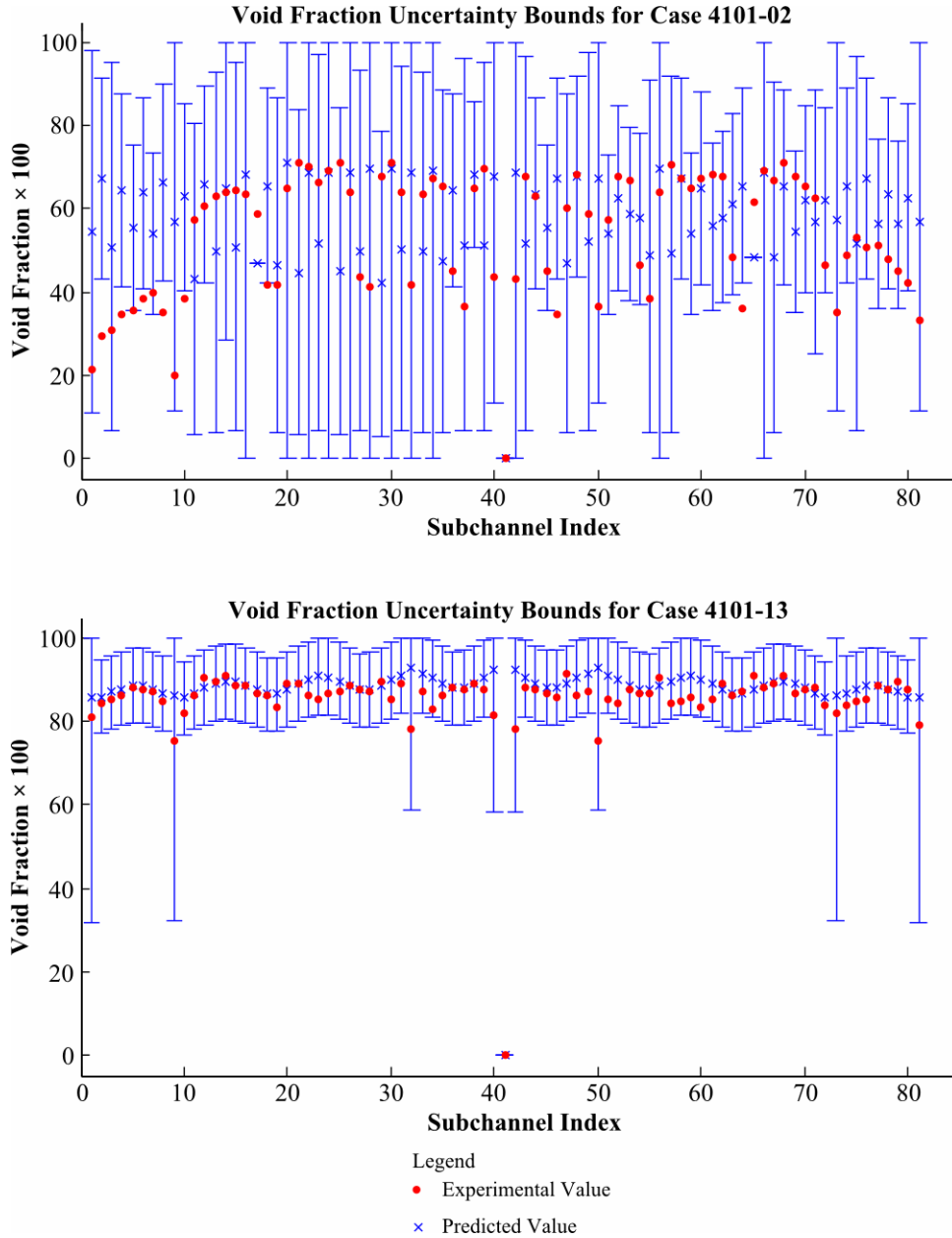


Figure 2. Uncertainty bounds for low pressure cases.

Case 4101-02 is characterized by a set of boundary conditions with low pressure, power and flow. The experimental void fraction in this case ranges between 0.20 to 0.71, and Figure 2 and Figure 4 illustrate that the developed RELAP5 model (nodalization plus RELAP5 code) has difficulty predicting the void fraction under these conditions. On average, the difference between the experimental and simulated points was 0.19 - in terms of void fraction for this particular case. The large uncertainty bounds represent the fact that the inaccurate predictions are common among cases run under similar conditions using the current nodalization and code.

In cases 4101-13 and 4101-86, the uncertainty bands in subchannels 1, 9, 72 and 81 (corner channels) are noticeably larger. These subchannels are only adjacent to one-quarter of one of the fuel rods meaning that the subchannel power to mass flux ratio is lower, forcing the data points from those subchannels to be classified in a different hypercube.

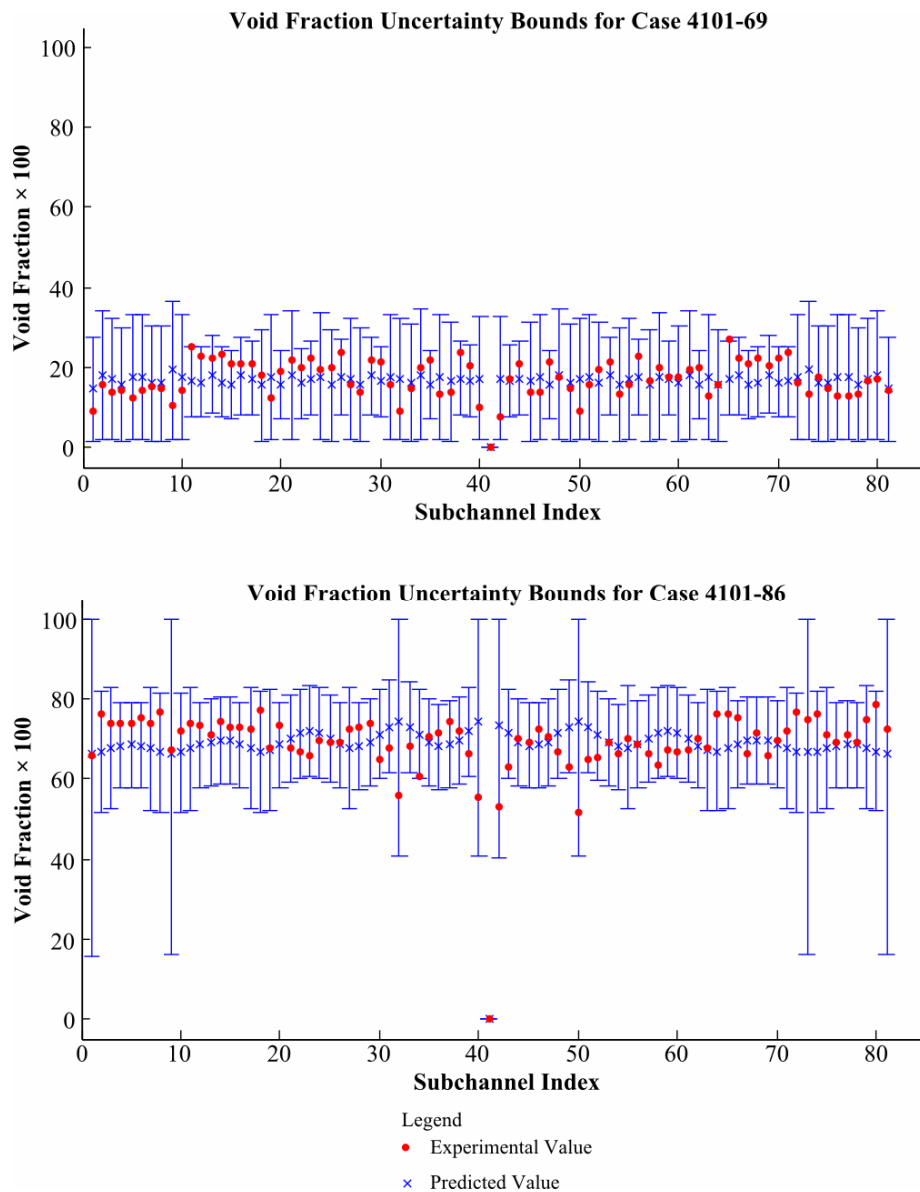


Figure 3. Uncertainty bounds for high pressure cases.

In the same two cases, subchannels 32, 40, 42 and 50 also stand out as they are only adjacent to two fuel rods with a relative power factor of 0.89. This puts them in a different hypercube than surrounding subchannels. Since the code is consistent in over-predicting the void in these channels, the accuracy quantities associated with these channels is higher, which in turn causes the uncertainty bands to be larger.

In both of the high power cases, 4101-13 and 4101-86, all experimental points fell within the predicted uncertainty bounds. In case 4101-69 - the low power, high pressure test - the uncertainty bounds encompassed all but one of the experimental points. In case 4101-02 - low power, flow and pressure - 87.5% of the experimental points fell within the predicted bounds, although very large uncertainty bands were required to accomplish this. Additionally, two points from this case were classified to empty hypercubes, thus no uncertainty bands were predicted.

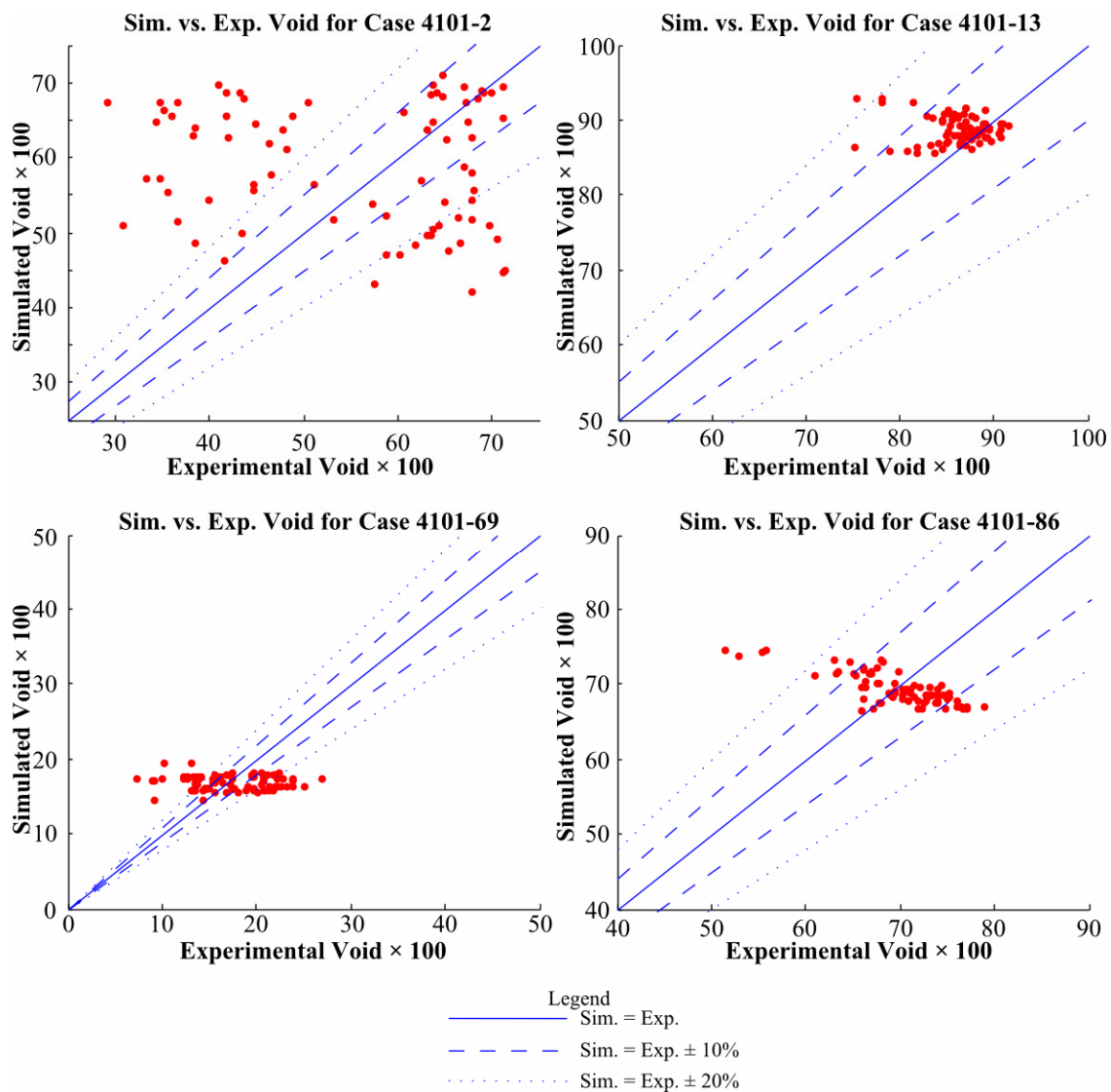


Figure 4. Predicted versus measured plots for the test cases.

Table IV. Accuracy Quantification of Selected Cases

	Test			
	4101-02	4101-13	4101-69	4101-86
Predicted Planar Void Fraction Average	0.589	0.887	0.168	0.693
Experimental Planar Void Fraction Average	0.541	0.863	0.173	0.697
Sample Averaged Bias Error	0.191	0.029	0.043	0.003
Sample Averaged Absolute Bias Error	0.338	0.036	0.240	0.081
Maximum Bias Error	1.852	0.230	1.323	0.447
Predicted Void Fraction Standard Deviation	0.075	0.014	0.009	0.017
Experimental Void Fraction Standard Deviation	0.127	0.025	0.035	0.037
Coverage Ratio	0.100	0.588	0.050	0.250

A summary of the test results is provided in Table IV, while predicted versus measured plots are illustrated in Figure 4. On an aggregate level, the planar void fraction averages at the top of the simulated bundle are in close agreement with the experimental void averages: the differences between the four predicted averages values and the experimental values are less than 0.05 (in absolute terms). This implies that for the sets of boundary conditions tested, the code is capable of predicting the correct quantity of vapour in the bundle. However it is evident that the distribution of the vapour among the subchannels is not accurately predicted.

The simulations exhibit a lower standard deviation than the experiment, which suggests that the void profile is more uniform than in the experiment. This is believed to be caused by a high level of mixing in between the subchannels, although work to verify this is still ongoing. Also notable is the sample bias error for test 4101-02 which is an order of magnitude larger than that of the other tests.

The coverage ratio as defined by the BFBT specifications in Table II has limited applicability when the experimental void fraction is low. In case 4101-69, the coverage ratio suggests that only 4 out of the 80 points fell within 3% of the experimental value. However, as the experimental average void fraction is 0.174, this means only the simulated values that fall within 0.005 contribute to the coverage ratio. If we moved away from defining the error in terms of a ‘percent of a percent’, and consider counting all the subchannel void fractions that satisfied the condition $|\alpha^{\text{code}} - \alpha^{\text{exp}}| \leq 0.03$ instead of $|\alpha^{\text{code}} - \alpha^{\text{exp}}| \leq 0.03\alpha^{\text{exp}}$, then we would find that 42.5% of the points in this particular case were covered.

5. CONCLUSIONS

This paper has demonstrated how the CIAU methodology proposed by the University of Pisa can be easily modified to predict uncertainty bands on void fraction simulations at the subchannel level. The proposed methodology has been successfully tested against 4 cases of the BFBT benchmark: the predicted uncertainty bands encompass the experimental data points in all four test cases except for about 12% of data in the test 4101-02.

The methodology fully relies on the availability of experimental data used for generating the accuracy and uncertainty database. The produced uncertainty bands are affected by the level of accuracy of the predicted calculations: a large discrepancy between predicted and experiments values in the tests used for developing the database reflect in a large size of the uncertainty bands when the method is applied to the tests case of interest.

REFERENCES

1. B. Neykov, F. Aydogan, L. Hochreiter, K. Ivanov, H. Utsuno, K. Fumio, *NUPEC BWR Full-Size Fine-Mesh Bundle Test (BFBT) Benchmark. Volume 1: Specifications*, NEA/NSC/DOC(2005)5.
2. F. Aydogan, L. Hochreiter, K. Ivanov, M. Martin, H. Utsuno, E. Satori, *NUPEC BWR Full-Size Fine-Mesh Bundle Test (BFBT) Benchmark. Volume II: Uncertainty and Sensitivity Analyses of Void Distribution and Critical Power - Specification*, NEA/NSC/DOC(2007)21
3. A. Kovtonyuk, A. Petruzzi, C. Parisi, F. D'Auria, "RELAP5-3D© Analysis of OECD-NEA NRC BFBT Benchmark", *NURETH12*, Pittsburgh, Sept 30 – Oct 4, 2007
4. *RELAP5-3D© Code Manuals, Appendix A*, Idaho National Engineering and Environmental Laboratory, INEEL-EXT-98-00834, Revision 2.4, 2006.
5. F. D'Auria, W. Giannotti, "Development of Code with capability of Internal Assessment of Uncertainty", *J. Nuclear Technology*, **131**, No. 1, pp 159-196 (2000).
6. A. Petruzzi, F. D'auria, W. Giannotti, K. Ivanov , "Methodology of Internal Assessment of Uncertainty and Extension to Neutron-Kinetics/Thermal-Hydraulics Coupled Codes", *Nuclear Science and Engineering*, **149**, pp 1-26, (2005).